



HAL
open science

Impact of Strong Scattering Resonances on Ballistic and Diffusive Wave Transport

Benoit Tallon, Thomas Brunet, John H Page

► **To cite this version:**

Benoit Tallon, Thomas Brunet, John H Page. Impact of Strong Scattering Resonances on Ballistic and Diffusive Wave Transport. *Physical Review Letters*, 2017, 119 (16), pp.164301. 10.1103/PhysRevLett.119.164301 . hal-03817599

HAL Id: hal-03817599

<https://hal.science/hal-03817599>

Submitted on 17 Oct 2022

HAL is a multi-disciplinary open access archive for the deposit and dissemination of scientific research documents, whether they are published or not. The documents may come from teaching and research institutions in France or abroad, or from public or private research centers.

L'archive ouverte pluridisciplinaire **HAL**, est destinée au dépôt et à la diffusion de documents scientifiques de niveau recherche, publiés ou non, émanant des établissements d'enseignement et de recherche français ou étrangers, des laboratoires publics ou privés.

Impact of Strong Scattering Resonances on Ballistic and Diffusive Wave Transport

Benoit Tallon and Thomas Brunet*

I2M, Université de Bordeaux—CNRS—Bordeaux INP, Talence F-33405, France

John H. Page

Department of Physics, University of Manitoba, Winnipeg, Manitoba, Canada R3T 2N2

(Received 24 July 2017; published 19 October 2017)

The strong impact of scattering resonances on *all* the key transport parameters of classical waves in disordered media is demonstrated through ultrasonic experiments on monodisperse emulsions. Through accurate measurements of both ballistic and diffusive transport over a wide range of frequencies, we show that the group velocity is large near sharp resonances, whereas the energy velocity (as well as the diffusion coefficient) is significantly slowed down by resonant scattering delay. Excellent agreement between theory and experiment is found, elucidating the effects of resonant scattering on wave transport in both acoustics and optics.

DOI: 10.1103/PhysRevLett.119.164301

During the last two decades, classical wave transport through strongly resonant scattering media has gained renewed interest in the field of wave physics [1]. Numerous experimental and theoretical investigations have been reported on various model systems of disordered resonant scatterers in optics [2–5] and in acoustics [6–11]. In such systems, the scatterers can support shape resonances (called Mie resonances in optics [12]) which may strongly influence the characteristic velocities of wave transport in random media [1]. As has been known for a long time [13], the group velocity (v_{gr}), which characterizes the coherent, ballistic propagation of a pulse straight through the medium [14], has to be distinguished from the energy velocity (v_e) of the dominant diffusive waves, which corresponds to the average local velocity of energy transport in the diffusion process. The energy velocity v_e is related to the wave diffusion coefficient D by $D = v_e \ell^*/3$, with ℓ^* being the transport mean free path, which is the average distance after which wave propagation is fully randomized.

One of the difficulties in the experimental observation of resonant behavior in both group and energy velocities in strongly scattering media is that diffusive transport becomes fully developed only after several transport mean free paths ℓ^* , while the ballistic component tends to vanish for such large propagation distances. To have a reasonable prospect of success in measuring v_{gr} and v_e , model systems of disordered resonant scatterers are required, such as random powders of monodisperse TiO_2 spheres as reported in optics [5] or glass bead suspensions in acoustics [7]. The group and energy velocities were found to be very similar in magnitude and frequency dependence in this typical acoustic system [7], whereas v_{gr} and v_e were predicted to be very different for optical systems [2], with small values of v_e being found experimentally relative to an estimate of

v_{gr} [5]. These strikingly different results may be due to differences in the refractive index contrast: in optical experiments, the refractive index n of the scattering particles is greater than 1 ($n_{\text{opt}} = 2.5$ for TiO_2 particles [5]) whereas in the acoustic experiments the refractive index n of the particles relative to the surrounding medium [15] is normally smaller than 1 ($n_{\text{ac}} = 0.3$ for SiO_2 beads in water [7]). Are optical and acoustical systems always so different? Can ultrasonic techniques be harnessed to reveal complementary information on the effects of strong and narrow scattering resonances on wave transport?

In this Letter, we address these questions through ultrasonic experiments on a system of disordered monodisperse resonant droplets having a high acoustic refractive index relative to the embedding medium. Thus, we are able to study the acoustic analogue of Mie scattering resonances in optics while capitalizing on the advantages of ultrasonic techniques that allow the simultaneous measurement of both ballistic and diffuse contributions to the total wave transport. This is possible because the use of phase sensitive detectors in acoustics allows the time dependence of both the average wave field and the average intensity to be measured in pulsed experiments, enabling the most comprehensive experimental investigation so far of a multiply scattering system with strongly scattering resonances analogous to those encountered in optics. Measurements of the scattering mean free path and phase velocity confirm that strong resonant scattering occurs in our acoustic system. Near resonances (identified by dips in the scattering mean free path), there are sharp peaks in the frequency dependence of the group velocity, and dips in diffusion coefficient and energy velocity, providing the first clear experimental evidence that v_{gr} is much larger than v_e (by as much as 3 times) near the strongest resonances of high refractive index inclusions. The data

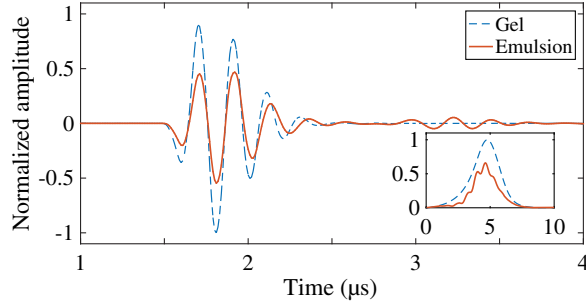


FIG. 1. Ballistic pulse transmitted through the emulsion (solid red curve) and a reference pulse through gel (dashed blue curve) for a propagation distance $z = 2$ mm. The inset shows the normalized FFT magnitudes versus frequency.

are well explained with rigorous theoretical models that show clearly the role of resonant scattering delay in determining the slow diffusive transport in this strongly resonant scattering system.

Our “resonant emulsions” are made of fluorinated oil (FC40) droplets randomly dispersed in a water-based gel matrix. This model system of disordered resonant scatterers has many advantages: (i) the all-fluid structure of these emulsions allows the acoustic (scalar) field to be directly measured within the sample, something that is not possible with solid materials usually considered in studies of wave transport; (ii) these random media exhibit a large sound-speed contrast between the scatterers ($v_1 \equiv v_{\text{oil}} = 0.64$ mm/μs) and the surrounding medium ($v_0 \equiv v_{\text{gel}} = 1.48$ mm/μs), giving a high refractive index $n_{\text{oil}} = 2.3$ relative to gel and enhancing the droplet resonances [16]; (iii) intrinsic losses within the components of our emulsions (oil and gel) are quite negligible in the MHz range investigated in this study, enabling the diffusive waves to be studied over a long range of times [17]; (iv) robotics used for the fabrication of our resonant emulsions enables samples with very low polydispersities ($\sim 3\%$) to be produced, a sample attribute that is crucial for clearly observing Mie resonances [18,19]. Furthermore, since we only consider dilute emulsions with low volume fractions ϕ ($\sim 5\%$) in this study, the use of the independent scattering approximation (ISA) [1] should be appropriate for interpreting our experimental data.

Ballistic measurements were performed by immersing two identical broadband ultrasonic transducers in the pure gel matrix (to obtain a reference pulse through a known material), and then in the emulsion (to measure the coherent wave transmitted through the emulsion)—see Fig. 1. This configuration ensured that the ballistic pulse could be accurately measured by taking advantage of the spatial averaging of the acoustic field across the large surface area of the receiver (1-in. diameter, corresponding to a spatial average over more than 1500 speckles at 2.5 MHz). Measurements over several configurations of disorder confirmed that the complex shape of this broadband pulse

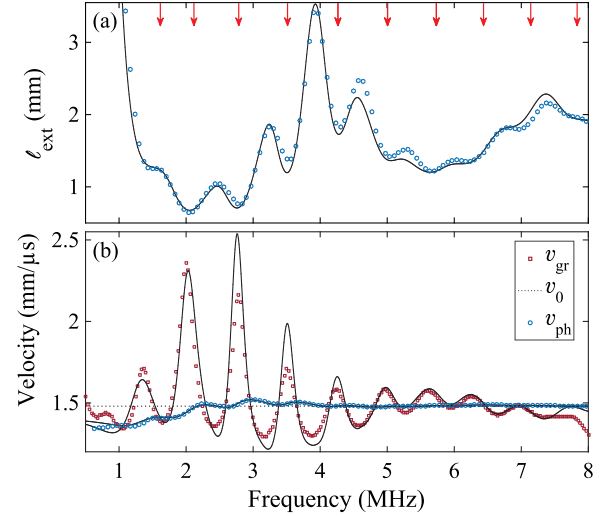


FIG. 2. (a) Measured extinction length $\ell_{\text{ext}} (\approx \ell_s)$, (b) phase velocity v_{ph} and group velocity v_{gr} (circles and squares, respectively), compared to the phase velocity $v_0 (=1.48$ mm/μs) in the pure water-based gel matrix (dotted line). Theoretical calculations are based on the independent scattering approximation (solid lines). Red arrows indicate the resonant frequencies of isolated fluorinated-oil droplets with $a = 170$ μm. For this emulsion, the polydispersity was 3%.

shown in Fig. 1 (including the oscillations in its tail) is due to dispersion and not to residual (imperfectly cancelled) incoherent signal. The frequency-resolved extinction length ℓ_{ext} [Fig. 2(a)], which is essentially equal to the scattering mean free path ℓ_s since dissipation is so small in our emulsions [20], and the phase velocity v_{ph} [Fig. 2(b)] were determined from the ratio of the complex fast Fourier transforms (FFTs) of the ballistic and reference waves. The group velocity v_{gr} , shown in Fig. 2(b), was determined by first numerically filtering the transmitted pulses with a narrow band Gaussian filter ($\Delta f = 20$ kHz) around many different central frequencies (from 0.5 MHz to 8 MHz) and then deducing v_{gr} from the time shifts of the pulse envelope maxima for each frequency [14,21].

The strong frequency dependence of these ballistic parameters reveals the highly resonant behavior of our emulsion, in which the sharp acoustic (Mie-type) resonances are associated with low values of ℓ_{ext} and with large variations of v_{ph} as shown in Fig. 2. Remarkably good agreement was found between our measurements and the theoretical predictions based on the ISA including the measured droplet-size distribution of our sample:

$$k^2 = (k' + jk'')^2 = k_0^2 + \int_a 4\pi\eta f(0) da. \quad (1)$$

Here $\eta = 3\phi/(4\pi a^3)$ is the number of scatterers per unit volume, a is the droplet radius, and $f(0)$ is the forward scattering amplitude of a single droplet, defined in terms of the scattering coefficients A_m as $f(0) = (1/jk_0) \sum_{m=0}^{\infty} (2m+1)A_m$ [18]. From the real and

imaginary parts of the wave number k' and k'' , v_{ph} ($k' = \omega/v_{\text{ph}}$), $v_{\text{gr}} = \partial\omega/\partial k'$, and $\ell_{\text{ext}} (=1/2k'')$ were determined.

In the vicinity of the strongest resonances (between 1.5 and 3.5 MHz), $\ell_s (\approx \ell_{\text{ext}})$ is short and comparable with the wavelength $\lambda (= v_{\text{ph}}/f)$, so that the coherent wave becomes vanishingly small relative to the diffusive waves. When $L \gg \ell^*$, wave transport becomes purely diffusive [6,8,22]. The diffusion coefficient D was characterized through frequency-, time-, and position-resolved experiments by measuring the temporal evolution of the diffusive halo, as done previously in glass bead suspensions [6]. The incoherent field generated by a point source at the input face of the sample ($z = 0, \rho = 0$) was measured by a needle hydrophone in different single speckle spots at positions ($z > 0, \rho$) in the emulsion, which was shaped as a circular slab of thickness $L = 26$ mm. After numerical filtering (in order to obtain frequency resolved results), the squared envelopes of the codas were calculated and ensemble averaged by taking advantage of the spatial ergodicity of our ultrasonic setup. Since our experiments were performed inside the emulsion, this quantity is proportional to the energy density U , unlike the usual situation in acoustics and optics in which the detector is placed outside the sample and the transmitted (or reflected) flux is measured [6,11,22]. Thus, we were able to measure the energy density inside the sample for fixed z at several transverse distances ρ from the source axis, and determine the off-axis/on-axis ratio $U(\rho, t)/U(0, t) = \exp[-\rho^2/(4Dt)]$. From this ratio, the transverse width squared of the diffuse halo $w^2(t) = 4Dt$ provides a direct measure of D , without complications due to absorption or boundary conditions [6].

Figure 3 shows representative experimental results obtained using a broadband pulsed point source centered at 2.8 MHz to observe the effects of the strongest resonances. The measured coda [Fig. 3(a)] is the signature of multiple scattering paths, which are clearly visible for long times up to 1000 μs . Figures 3(b) and 3(c) show $U(\rho, t)$ and $w^2(t)$ for frequencies near 2.7 MHz. These measurements were performed at a depth $z = 20$ mm. From a linear fit to $w^2(t)$ [Fig. 3(c)], we obtain an accurate measurement of $D = 0.40 \pm 0.01$ $\text{mm}^2/\mu\text{s}$ at this frequency. For $U(\rho, t)$ [Fig. 3(b)], the solid black lines show the predictions of diffusion theory, taking into account the finite-thickness L of the slab and absorption [23]; note that only two fitting parameters are needed: U_0 , the initial energy density, and τ_a , the absorption time. The known (fixed) input parameters were D [measured from $w^2(t)$], the internal reflection coefficient (calculated from the ballistic parameters [6,24,25]), and ℓ^* [estimated from the measured values of ℓ_s using $\ell^* = \ell_s/(1 - \langle \cos \theta \rangle)$, where $\langle \cos \theta \rangle = \int_0^\pi \cos \theta |f(\theta)|^2 \sin \theta d\theta / \int_0^\pi |f(\theta)|^2 \sin \theta d\theta$ is the weighted average of $\cos \theta$ over scattering angles θ]. The excellent agreement between the measured and calculated energy density profiles in Fig. 3(b), for all distances ρ , shows that

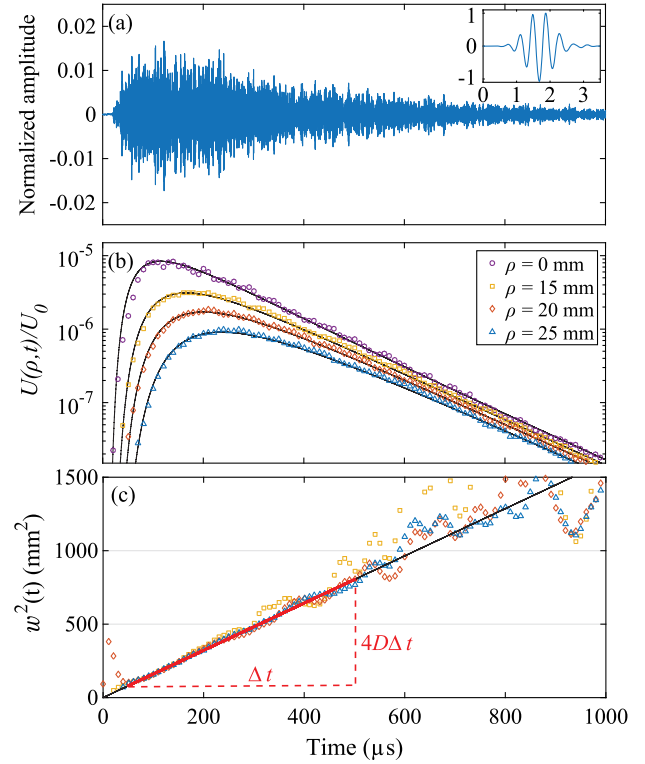


FIG. 3. (a) Transmitted unfiltered incoherent field for one realization of disorder (at $\rho = 0$ mm and $z = 20$ mm), with the input signal shown in the inset. (b) Average energy density (normalized by the incident energy density U_0) for different transverse distances ρ after numerical filtering of transmitted codas around $f_0 = 2.7$ MHz. (c) The linear fit of the width squared of the diffuse halo between 50 and 500 μs (red line) provides an accurate measurement of the diffusion coefficient D . In (b) and (c), symbols denote experimental data and the black lines correspond to the theoretical predictions over all times up to 1000 μs .

diffusion theory describes the data very well and further validates the measurement of D .

This procedure was repeated for each filtering frequency (from 1 MHz to 3.6 MHz) to obtain frequency-dependent measurements of both D [Fig. 4(a)] and τ_a [Fig. 4(b)]. The absorption time τ_a in the emulsion was found to be around 5 times shorter than the intrinsic absorption time τ_0 in the pure gel matrix, with the increased absorption likely due to viscous losses at the interface between the oil droplets and the gel matrix [26,27].

The low values of D and its frequency dependence are strongly influenced by scattering resonances. This behavior can be understood by examining the energy velocity v_e , which can be determined from the measured values of D and the estimated ℓ^* since $v_e = 3D/\ell^*$. The energy velocity v_e was then compared to the group velocity v_{gr} as shown in Fig. 5. Contrary to what was observed in concentrated suspensions of glass beads at ultrasonic frequencies [7], v_e here is very different in magnitude and frequency dependence to v_{gr} . This difference may be

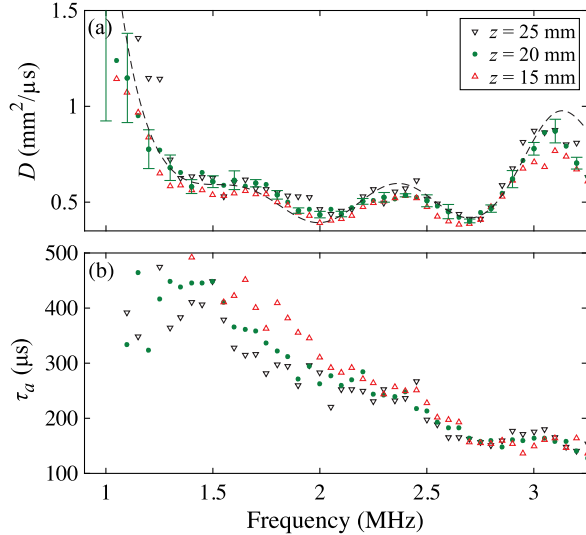


FIG. 4. (a) Measured diffusion coefficient D as a function of frequency (symbols) from the fits for $w^2(t)$ [cf. Fig. 3(c)], compared with theoretical predictions from the independent scattering approximation (dashed lines). (b) Absorption time τ_a deduced from the fits for $U(\rho, t) \propto \exp(-t/\tau_a)$ [cf. Fig. 3(b)]. The experimental data shown here were obtained from measurements done for three different depths z ($=15, 20,$ and 25 mm) within the sample.

attributed to the different character of the scattering resonances in these two cases. For the emulsion, the low values of v_e and anomalously high values of v_{gr} are reminiscent of predictions in optics for strongly scattering TiO_2 particles [2,28]. For the scalar wave case relevant to acoustic waves in emulsions, these predictions for v_e can be conveniently written as

$$v_e = \frac{v_0^2/v_{ph}}{1 + \delta}, \quad \text{with} \quad (2)$$

$$\delta = 2\pi\eta v_{gr} \left(\frac{v_{ph}}{\omega} \frac{\partial \text{Re}f(0)}{\partial \omega} + \int_0^\pi \sin\theta |f(\theta)|^2 \frac{\partial \varphi}{\partial \omega} d\theta \right), \quad (3)$$

where φ is the phase of the scattering amplitude $f(\theta)$ [29]. The first term in δ accounts for the influence of the group velocity, while the second term is proportional to the scattering delay due to resonant trapping of energy in the droplets. These terms are of opposite sign, with the (positive) scattering delay term being dominant, thereby causing the energy velocity to be small compared with v_0 and v_{gr} , especially near the strongest resonances at $f = 2$ MHz and 2.7 MHz. This model, in which there are no adjustable parameters, is in very good agreement with our data for v_e , as shown in Fig. 5. In combination with our results for ℓ^* , it also enables the frequency dependence of D to be accurately predicted [Fig. 4(a)].

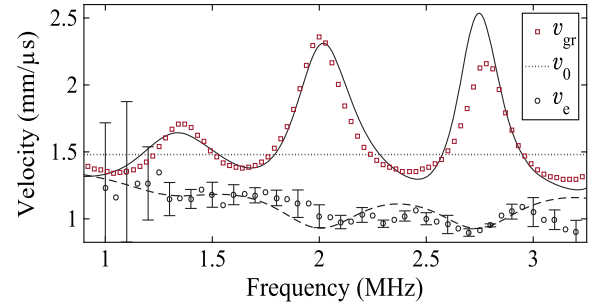


FIG. 5. Comparison of the energy and group velocities from the experiments (circles and squares, respectively) and theory (dashed and solid lines). The sound speed in the pure gel matrix is represented by the dotted line.

In conclusion, we have obtained a complete set of experimental data for the key transport parameters of a strongly scattering medium composed of monodisperse resonant droplets. We find that the group velocity differs significantly from the energy velocity in the vicinity of the scattering resonances. Such behavior is unusual in acoustics and is due to the high relative refractive index of the droplets. Our data are well explained by theoretical calculations that take into account the strong dispersion of the coherent wave and the pronounced scattering delay experienced by the diffusive waves. In particular, the all-fluid structure of our emulsions, which only support the propagation of longitudinal waves, allows a direct validation of scalar wave theories for v_e , which have not been tested directly in a purely scalar wave system previously. Furthermore, our precise measurements of both v_{gr} and v_e show conclusively that $v_e \ll v_{gr}$ near the resonances of high index inclusions, as are encountered in optics where accurate measurements of v_{gr} in strongly scattering diffusive media have been elusive. Finally, we note that the strong scattering exhibited in our emulsions suggests that, at higher concentrations of droplets where interference effects would be expected to be important, resonant emulsions might be model systems for investigating the Anderson localization acoustic waves, thereby complementing previous experiments on mesoglasses at ultrasonic frequencies [30–34].

This work was supported by the LabEx AMADEus (ANR-10-LABX-42) within IdEx Bordeaux (ANR-10-IDEX-03-02), i.e., the Investissements d’Avenir programme of the French government managed by the Agence Nationale de la Recherche, and the Natural Sciences and Engineering Research Council of Canada’s Discovery Grant Program (RGPIN-2016-06042).

*thomas.brunet@u-bordeaux.fr

[1] P. Sheng, *Introduction to Wave Scattering, Localization, and Mesoscopic Phenomena* (Springer-Verlag, Berlin, 2006).

- [2] M. P. van Albada, B. A. van Tiggelen, A. Lagendijk, and A. Tip, *Phys. Rev. Lett.* **66**, 3132 (1991).
- [3] E. Kogan and M. Kaveh, *Phys. Rev. B* **46**, 10636 (1992).
- [4] K. Busch, C. M. Soukoulis, and E. N. Economou, *Phys. Rev. B* **52**, 10834 (1995).
- [5] R. Sapienza, P. D. García, J. Bertolotti, M. D. Martín, A. Blanco, L. Viña, C. Lopez, and D. S. Wiersma, *Phys. Rev. Lett.* **99**, 233902 (2007).
- [6] J. H. Page, H. P. Schriemer, A. E. Bailey, and D. A. Weitz, *Phys. Rev. E* **52**, 3106 (1995).
- [7] H. P. Schriemer, M. L. Cowan, J. H. Page, P. Sheng, Z. Liu, and D. A. Weitz, *Phys. Rev. Lett.* **79**, 3166 (1997).
- [8] A. Derode, A. Tourin, and M. Fink, *Phys. Rev. E* **64**, 036605 (2001).
- [9] M. L. Cowan, J. H. Page, and P. Sheng, *Phys. Rev. B* **84**, 094305 (2011).
- [10] T. Brunet, K. Zimny, B. Mascaró, O. Sandre, O. Poncelet, C. Aristégui, and O. Mondain-Monval, *Phys. Rev. Lett.* **111**, 264301 (2013).
- [11] N. Viard and A. Derode, *J. Acoust. Soc. Am.* **138**, 134 (2015).
- [12] G. Mie, *Ann. Phys. (Berlin)* **330**, 377 (1908).
- [13] A. Lagendijk and B. A. van Tiggelen, *Phys. Rep.* **270**, 143 (1996).
- [14] J. H. Page, P. Sheng, H. P. Schriemer, I. Jones, X. Jing, and D. A. Weitz, *Science* **271**, 634 (1996).
- [15] Unlike in optics, there is no reference medium, such as vacuum, to define an absolute acoustic refractive index. Here we have chosen water as a reference medium ($v_{\text{water}} = 1.48 \text{ mm}/\mu\text{s} [= v_{\text{gel}}]$) leading to a relative refractive index for acoustic waves: $n_{\text{ac}} = v_{\text{water}}/v_{\text{glass}}$ for glass relative to water and $n_{\text{ac}} = v_{\text{gel}}/v_{\text{oil}}$ for fluorinated oil relative to gel.
- [16] T. Brunet, S. Raffy, B. Mascaró, J. Leng, R. Wunenburger, O. Mondain-Monval, O. Poncelet, and C. Aristégui, *Appl. Phys. Lett.* **101**, 011913 (2012).
- [17] Intrinsic absorption times τ_0 and τ_1 in the pure water-based gel matrix and in the fluorinated oil FC40, respectively, were measured as a function of frequency f and found to vary as $\tau_0 = 7 \times 10^3 f^{-2} \mu\text{s}$ and $\tau_1 = 7 \times 10^2 f^{-2} \mu\text{s}$, with f in MHz.
- [18] B. Mascaró, T. Brunet, O. Poncelet, C. Aristégui, S. Raffy, O. Mondain-Monval, and J. Leng, *J. Acoust. Soc. Am.* **133**, 1996 (2013).
- [19] The importance of investigating samples with low polydispersity in order to clearly see the effects of the resonances was demonstrated in Ref. [18]. There it was shown, both experimentally and theoretically, that the resonant peaks in phase velocity and attenuation (inversely proportional to the extinction length) become progressively smoothed out as the polydispersity is increased, and are difficult to resolve for a polydispersity greater than about 13%.
- [20] In general, the extinction length includes both dissipation and scattering attenuation mechanisms since it is defined as $1/\ell_{\text{ext}} = 1/\ell_s + 1/\ell_a$ with ℓ_s the scattering mean free path and ℓ_a the absorption length ($v_{\text{gr}} \times \tau_a$). Using our measurements of v_{gr} and τ_a from ballistic and diffusive measurements, respectively [Figs. 2(b) and 4(b)], we estimate ℓ_a to be between 2 and 3 orders of magnitude greater than ℓ_s over the strong resonant frequency range from 1–3.5 MHz where τ_a was measured. Thus, the ballistic pulse extinction is almost entirely due to resonant scattering ($\ell_{\text{ext}} \approx \ell_s$).
- [21] M. L. Cowan, K. Beaty, J. H. Page, Z. Liu, and P. Sheng, *Phys. Rev. E* **58**, 6626 (1998).
- [22] Z. Q. Zhang, I. P. Jones, H. P. Schriemer, J. H. Page, D. A. Weitz, and P. Sheng, *Phys. Rev. E* **60**, 4843 (1999).
- [23] H. Carslaw and J. Jaeger, *Conduction of Heat in Solids* (Clarendon Press, Oxford, 1959).
- [24] H. P. Schriemer, Doctoral thesis, University of Manitoba, 1997.
- [25] J. X. Zhu, D. J. Pine, and D. A. Weitz, *Phys. Rev. A* **44**, 3948 (1991).
- [26] D. J. McClements and M. J. W. Povey, *J. Phys. D* **22**, 38 (1989).
- [27] This interpretation is supported by the observation that minima of τ_a occur around resonances where droplet deformations are much higher (e.g., at 2.75 MHz in Fig. 4(b) for the quadrupolar resonance).
- [28] B. A. van Tiggelen, A. Lagendijk, M. P. van Albada, and A. Tip, *Phys. Rev. B* **45**, 12233 (1992).
- [29] For weak resonances, Eqs. (2) and (3) reduce to the simpler form found in Ref. [7], in which the relationship between v_e and v_{gr} is particularly transparent.
- [30] H. Hu, A. Strybulevych, J. H. Page, S. E. Skipetrov, and B. A. van Tiggelen, *Nat. Phys.* **4**, 945 (2008).
- [31] S. Faez, A. Strybulevych, J. H. Page, A. Lagendijk, and B. A. van Tiggelen, *Phys. Rev. Lett.* **103**, 155703 (2009).
- [32] W. K. Hildebrand, A. Strybulevych, S. E. Skipetrov, B. A. van Tiggelen, and J. H. Page, *Phys. Rev. Lett.* **112**, 073902 (2014).
- [33] A. Aubry, L. A. Cobus, S. E. Skipetrov, B. A. van Tiggelen, A. Derode, and J. H. Page, *Phys. Rev. Lett.* **112**, 043903 (2014).
- [34] L. A. Cobus, S. E. Skipetrov, A. Aubry, B. A. van Tiggelen, A. Derode, and J. H. Page, *Phys. Rev. Lett.* **116**, 193901 (2016).